

Probabilistic Models to Evaluate Effectiveness of Steel Bridge Weld Fatigue Retrofitting by Peening

Scott Walbridge, Dilum Fernando, and Bryan T. Adey

The purpose of this study was to evaluate, with two probabilistic analytical models, the effectiveness of several alternative fatigue management strategies for steel bridge welds. The investigated strategies employed, in various combinations, magnetic particle inspection, gouging and rewelding, and postweld treatment by peening. The analytical models included a probabilistic strain-based fracture mechanics model and a Markov chain model. For comparing the results obtained with the two models, the fatigue life was divided into a small, fixed number of condition states based on crack depth, similar to those often used by bridge management systems to model deterioration due to other processes, such as corrosion and road surface wear. The probabilistic strain-based fracture mechanics model was verified first by comparison with design $S-N$ curves and test data for untreated welds. Next, the verified model was used to determine the probability that untreated and treated welds would be in each condition state in a given year; the probabilities were then used to calibrate transition probabilities for a much simpler Markov chain fatigue model. Then both models were used to simulate a number of fatigue management strategies. From the results of these simulations, the performance of the different strategies was compared, and the accuracy of the simpler Markov chain fatigue model was evaluated. In general, peening was more effective if preceded by inspection of the weld. The Markov chain fatigue model did a reasonable job of predicting the general trends and relative effectiveness of the different investigated strategies.

Bridge managers currently have a range of analytical tools at their disposal to facilitate maintenance planning for bridges subjected to deterioration due to various manifest processes, which can be readily observed and characterized over time, such as corrosion and road surface wear. In the case of fatigue deterioration, however, which is highly random in nature and may be difficult to detect for much of the life of the structure, a need remains for the development of similar tools that can be easily integrated with existing bridge management systems (BMSs), used to perform rapid analyses for large numbers of structures, and updated to model weld inspection and retrofitting events.

S. Walbridge, Department of Civil and Environmental Engineering, University of Waterloo, 200 University Avenue West, Waterloo, Ontario N2L 3G1, Canada. D. Fernando and B. T. Adey, Department of Structural, Environmental, and Geomatic Engineering, Institute of Construction and Infrastructure Management, ETH Zürich, Wolfgang-Pauli-Strasse 15, 8093 Zürich, Switzerland. Corresponding author: S. Walbridge, swalbrid@uwaterloo.ca.

Transportation Research Record: Journal of the Transportation Research Board, No. 2285, Transportation Research Board of the National Academies, Washington, D.C., 2012, pp. 27–35.
DOI: 10.3141/2285-04

In many existing BMSs the condition of a bridge or bridge element is characterized in terms of a distinct set of possible condition states (CSs) and possible transitions from one CS to another. The time period that the element will stay in each CS is then estimated on the basis of prediction models for the applicable deterioration mechanisms, available inspection data, or expert opinions.

Most existing BMSs identify fatigue damage of critical sections on the basis of inspection results and use criticality identification mechanisms [e.g., smart flags in PONTIS (1)] to highlight the necessity for actions against fatigue damage. Some advanced BMSs make predictions of the deterioration of elements due to fatigue damage by specifying discrete CSs based on fatigue cracking and using mechanistic or historical data-based models to predict the fatigue deterioration. For example, JH-BMS uses the formula of Higashiyama and Matsui (2) to predict fatigue damage of reinforced concrete slabs (3) and the fatigue assessment formula of the Japan Road Association to assess fatigue damage of the main members of a steel bridge (3). Often the fatigue damage prediction models used in existing BMSs are applied at the element level and are deterministic in nature [e.g., JH-BMS Matsui's formula (2)]. Probabilistic models would be an improvement over these deterministic ones, particularly if they could be used within the modeling framework of existing advanced BMSs [e.g., PONTIS (1), KUBA (4)].

For the retrofitting of fatigue-damaged welds, bridge managers have a range of options available, including member replacement, reinforcement, load restrictions, and increased monitoring, to name a few. Postweld treatments such as grinding, dressing, and peening are increasingly being considered as another possibility for the retrofitting of fatigue-damaged bridge welds. Fatigue testing has demonstrated the effectiveness of these treatments, and anecdotal reports of successful postweld treatment retrofits are increasing in number. Relatively sophisticated fatigue models are enabling the effectiveness of postweld treatments to be predicted with increased certainty as a function of the material properties, detail geometry, and loading. To date, however, there have been only limited attempts to model postweld treatment retrofits in a BMS framework, either for the purpose of maintenance planning or to predict the benefits of these treatments from a life-cycle cost perspective [e.g., the work by Orcesi et al. (5)].

Against this background, in the current study two probabilistic fatigue models are used to simulate several fatigue management strategies by employing postweld treatment by needle peening as one of the possible retrofitting methods. The two models are a probabilistic strain-based fracture mechanics (SBFM) model and a Markov chain fatigue model. To compare the two models, the fatigue life is divided into a small, fixed number of CSs based on

crack depth, similar to those often used by BMSs to model deterioration due to other processes. On the basis of the analysis results, the effectiveness of needle peening for the fatigue retrofitting of steel bridge welds is evaluated. In addition, from a comparison of the two models, the potential of the second model as a practical tool for bridge managers is evaluated and possibilities for improving this model are suggested.

Regarding the employed probabilistic fatigue models, a deterministic variant of Model 1 was shown by Ghahremani and Walbridge to be well suited for predicting the fatigue behavior of peened welds under in-service variable amplitude loading conditions (6). However, the potential for this model to be integrated into a BMS framework (by using either a deterministic or a probabilistic format) is thought to be limited because of its complexity and required calculation effort. Model 2 represents the first attempt known to the authors to model weld retrofitting by peening (for any structural application) with a Markov chain approach, which would lend itself well to integration into the currently available BMS software.

SBFM MODEL

The first of the two models employed in this study is a probabilistic version of a previously validated SBFM model. A full description of the deterministic model is given elsewhere (6). The basis for the model is the Paris–Erdogan crack growth law, commonly used for analysis with linear-elastic fracture mechanics (LEFM), modified to consider crack closure and the presence of a threshold stress intensity factor range. For the analysis of peened welds, as discussed by Ghahremani and Walbridge, the SBFM model offers considerable advantages over LEFM in terms of its ability to model the evolution of the residual stresses under variable amplitude loading histories (6). The main difference between LEFM and SBFM is the calculation of the stress intensity factor, K . In the SBFM model, the following expression is used:

$$K = Y \cdot E \cdot \varepsilon \cdot \sqrt{\pi \cdot a} \quad (1)$$

where

- ε = local strain at crack depth, a ;
- Y = correction factor to account for crack shape, free surface, and finite thickness of plate; and
- E = elastic modulus.

To calculate the stresses and strains for each load cycle, a Ramberg–Osgood material model is used (7), which requires as input the cyclic material parameters K' and n' . Strain histories at various depths below the surface of the weld toe are determined by using Neuber's rule (7) and crack closure is considered by using a model by Newman (8).

In the probabilistic version of the SBFM model, developed specifically for the current study, the various input parameters required by the model are replaced with statistical distributions. This approach has been used previously to perform probabilistic LEFM analysis of as-received and peened welds [e.g., by Walbridge and Nussbaumer (9)]. In the SBFM model, the additional parameters include the elastic modulus, E ; the static yield and ultimate strength, σ_y and σ_u ; the cyclic material parameters, K' and n' ; and an additional parameter, μ , which models the recovery of the crack opening stress following overloads.

Given the deterministic SBFM model from Ghahremani and Walbridge and statistical distributions for the various input parameters, Monte Carlo simulation can be used to generate histograms of failure probability versus imposed number of load cycles, N , for different treatment and loading conditions (6).

Cyclic Material Parameter Distributions

To estimate the uncertainties associated with the additional material parameters required to implement the probabilistic SBFM model (E , σ_y , σ_u , K' , n' , μ), a small database of material properties for structural steels was compiled from several sources (6, 10–12). This database included base metal, weld metal, and heat-affected zone data. A model is proposed by Baumel and Seeger for estimating K' and n' on the basis of σ_u (13). According to this model, K' can be taken as $1.65\sigma_u$ and used with a constant value for n' of 0.15.

When the database was examined, strong correlations were seen between σ_y and σ_u and the error in the K' and n' estimates with the use of the model from Baumel and Seeger (13). With this information, a linear relationship between σ_y and σ_u was assumed for estimating σ_u (see Figure 1), and $K'/(1.65\sigma_u)$ was taken as an initial estimate for $n'/0.15$. Statistical variables were then established to represent the estimation errors for each parameter. Statistical variables modeling the differences between the actual σ_y and E and the nominal values (based on the steel grade for σ_y , 200 GPa for E) also were assumed, on the basis of work by Schmidt and Bartlett (14).

Other Model Parameter Distributions

The other parameters required for the implementation of the probabilistic SBFM model were established on the basis of measurements (6) and review of the literature on probabilistic LEFM (see Table 1).

The following comments are made regarding these parameters:

- Different cyclic load and analysis uncertainty parameters [$\text{Var}(P_{\text{traffic}})$ and $\text{Var}(\text{SCF})$] are assumed to model laboratory fatigue tests (which have a relatively low uncertainty in the analysis and loading) and in-service conditions for welds in bridges.
- It is assumed that the fatigue verification procedure would be independent of the plate thickness (T) or yield strength (σ_y). Thus, uniform distributions are assumed for these parameters, covering a range of values likely to be seen in bridges.
- A uniform tensile residual stress due to welding, σ_{weld} , is assumed. The expected value is taken as 60% of σ_y (6). Needle peening is assumed to impose a compressive residual stress at the weld toe surface of 80% of σ_y , which gradually diminishes in magnitude up to a depth of ~ 1 mm (6). A key assumption made in the SBFM analysis is that residual stress modification is the only significant effect that needle peening has on the weld toe fatigue behavior. A fatigue life increase results because the compressive peening stresses reduce the growth rates of cracks less than ~ 1 mm in depth.

Model Verification with Design S – N Curves

The modeled fatigue detail was a Class C non-load-carrying transverse stiffener detail with a semielliptical crack propagating from the weld toe surface (15–17). For this detail, the elastic stress distribution along the crack path (required for the SBFM analysis) can

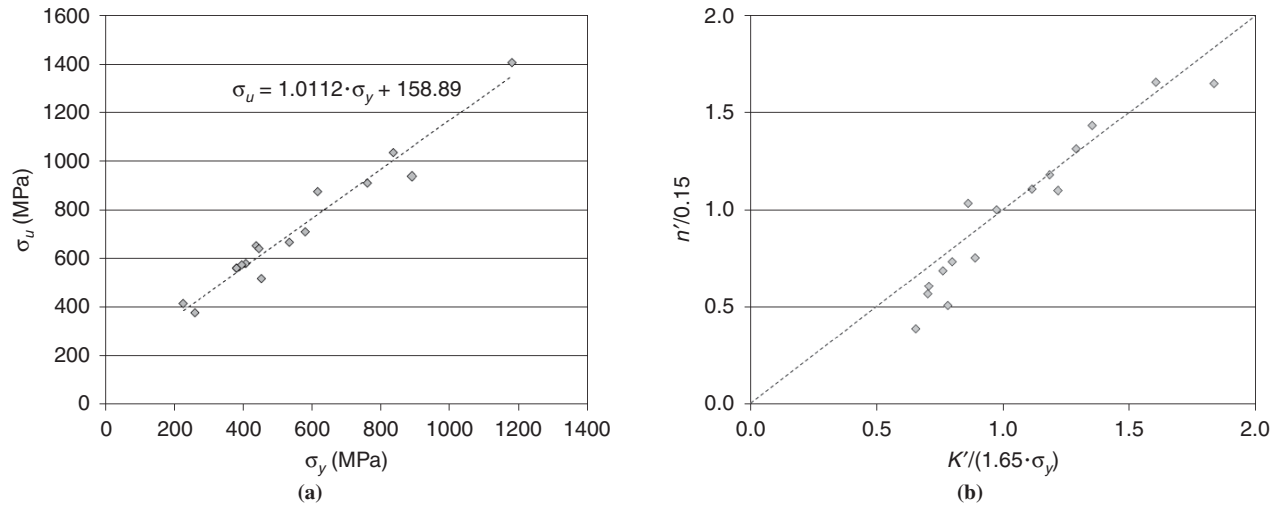


FIGURE 1 Data (6, 10–12) used to estimate (a) σ_u and (b) K' and n' given σ_y .

be estimated by using equations from Monahan (18), which require as input the plate thickness, T ; the weld toe angle, θ_w ; and the weld toe radius, ρ_w .

In order to verify the probabilistic SBFM model, an analysis was initially performed under constant amplitude loading at $\Delta S = 180$ MPa and $R (S_{min}/S_{max}) = 0.1$ for the as-welded case. The results are compared in Figure 2a with mean life and the 97.7% survival probability ($\mu - 2\sigma$) design $S-N$ curves (15–17). In Figure 2a, the SBFM model curves are plotted by fitting a straight line through the analysis results for $\Delta S = 180$ MPa with the same slope as the design

$S-N$ curves ($m = 3.0$). From Figure 2a, it can be seen that the mean life curve is closely predicted by the model.

The scatter (indicated by the spread between the mean life and the 97.7% survival probability curves) predicted by the model is greater than that indicated by the design curves. A likely explanation for this finding is that the data from Fisher et al. used to establish the design curves did not include the same plate thickness and yield strength ranges (19). In Figure 2b, the analysis results are compared with other test results performed by different laboratories for a larger range of steel grades (6, 20–22). This plot suggests that

TABLE 1 Probabilistic SBFM Analysis Variables

Variable	μ	σ	Units	Distribution	Description
a_i	0.15	0.045	mm	LN	Initial crack depth
$(a/c)_i$	0.50	0.16	—	LN	Initial crack aspect ratio
T	Range: 9.5–50.8		mm	Uniform	Nominal plate thickness
$\text{Var}(T)^a$	1.02	0.012	—	Normal	—
θ_w	39.8	6.9	°	LN	Weld toe angle
ρ_w	0.65	0.3	mm	LN	Weld toe radius
$\ln(C)$	-29.13	0.55	N, mm	normal	Paris law constant
ΔK_{th}	80.0	15.0	$\text{MPa} \cdot \sqrt{\text{mm}}$	LN	SIF range threshold
μ	0.002	0.001	—	LN	Crack closure parameter
$\text{Var}(E)^a$	1.04	0.026	—	Normal	E = elastic modulus
σ_y	Range: 345–690		MPa	Uniform	σ_y = yield strength
$\text{Var}(\sigma_y)^a$	1.07	0.053	—	LN	—
$\text{Var}(\sigma_u)^a$	1.0	0.077	—	LN	σ_u = ultimate strength
$\text{Var}(K')^a$	1.04	0.35	—	LN	K' = Ramberg–Osgood constant
$\text{Var}(n')^a$	0.92	0.15	—	LN	n' = Ramberg–Osgood constant
$\text{Var}(\sigma_{\text{weld}})^a$	1.0	0.25	—	Normal	σ_{weld} = welding residual stress
$\text{Var}(\sigma_{\text{pwt}})^a$	1.0	0.20	—	Normal	σ_{pwt} = peening residual stress
$\text{Var}(P_{\text{traffic}})^a$	1.0	0.15 (0.01 ^b)	—	Normal	P_{traffic} = traffic-induced load
$\text{Var}(\text{SCF})^a$	0.93 (1.0 ^b)	0.12 (0.02 ^b)	—	LN	SCF = stress concentration factor

NOTE: — = not applicable; ln = lognormal distribution; SIF = stress intensity factor.

^aVar() denotes multiplier applied to nominal or estimated value.

^bDenotes the value assumed for lab data analysis.

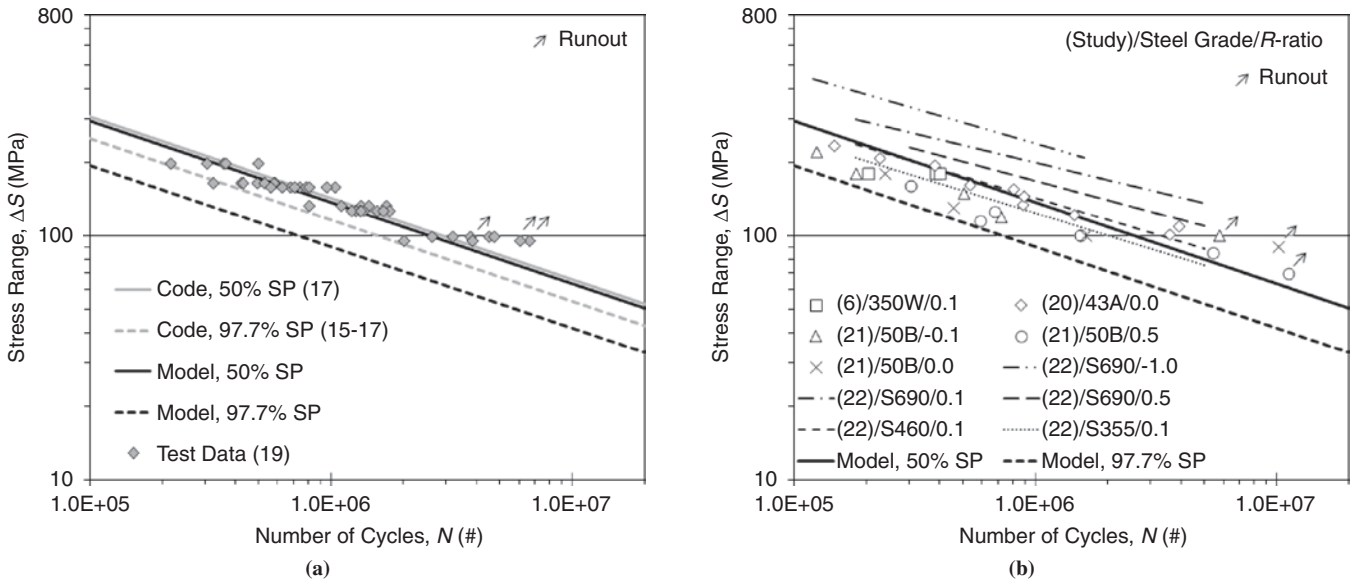


FIGURE 2 Comparison of probabilistic SBFM model results with (a) test data from Fisher et al. (19) and (b) test data from Ghahremani and Walbridge (6) and other sources (20–22).

the predicted scatter is not unreasonable when such a range of test results is considered.

Modeling of Inspection and Retrofitting

In the implementation of the model, the Paris–Erdogan crack growth law is integrated numerically over a crack depth range to get the fatigue life. In order to model inspection and retrofitting events at fixed times during the service life (e.g., based on a maintenance schedule), it is convenient to perform the integration in blocks of load cycles, N , of a predetermined size. In the current study, inspection is modeled based on work by Lassen, in which the following curve for probability of detection, P_D , is proposed (23):

$$P_D = P_0 \cdot (1 - \exp(-\gamma \cdot (a - a_0))) \quad (2)$$

where P_0 is the probability of detection for a large crack and a_0 is the smallest detectable crack size. $P_0 = 0.9$, $a_0 = 1.0$ mm, and $\gamma = 1$ are the values suggested by Lassen for magnetic particle inspection (23). In the current study, these values are used for illustrative purposes, and their variation to simulate other inspection methods is not considered.

Although visual inspection (which has a much different associated curve for probability of detection) is commonly used for routine assessment, when weld treatments are used for fatigue retrofitting, inspection by other methods, such as magnetic particle inspection, is normally required before the application of the treatment. For each trial in the Monte Carlo simulation, after a fixed number of cycles, N , the calculated crack size, along with Equation 2, can be used to determine if a crack has been detected. For the current study, false positives and errors in the crack size estimation are not considered. (This is an important simplifying assumption, since false positives can be significant for certain inspection methods.) If a crack is detected and exceeds a certain size, it will be repaired by gouging and rewelding. It is further assumed that this treatment will result in a repaired weld with an initial defect distribution the same as that

for a new weld. In addition to magnetic particle inspection, gouging, and rewelding, it is assumed that the residual stresses can be modified either before or after a given service period by needle peening. This retrofitting method is assumed to result in a modification of the assumed residual stress distribution along the crack path in the subsequent crack propagation steps (see Figure 3) but no modification to the crack depth itself.

MARKOV CHAIN FATIGUE MODEL

In addition to the probabilistic SBFM model, a much simpler Markov chain fatigue model is investigated, which has much stronger potential, in the view of the authors, for integration into a BMS framework. In fact, Markov chains are commonly used already to model deterioration of bridge elements due to other processes in BMSs (24). For this model, discrete CSs are defined and deterioration is modeled by estimating the probability, q_i , of passing from one CS to another in a fixed period of time. These transition probabilities are the elements of the transition probability matrix, P (25). In the current study, “unit jump” transition probability matrices (Table 2) are used; that is, it is assumed that the probability of jumping multiple CSs in one time increment is negligible.

At any given time, t :

$$p_t = p_{t-1} \cdot P \quad (3)$$

where p_t is a matrix containing the probabilities of being in each CS at time t . For the current study, it is assumed that there are a fixed number of traffic-induced load cycles, N , per year. Time increments of 1 year are assumed for the Markov chain analysis.

Definition of CSs

Table 3 provides the CS definitions assumed here for a weld subjected to fatigue loading. The use of Markov chains to model fatigue

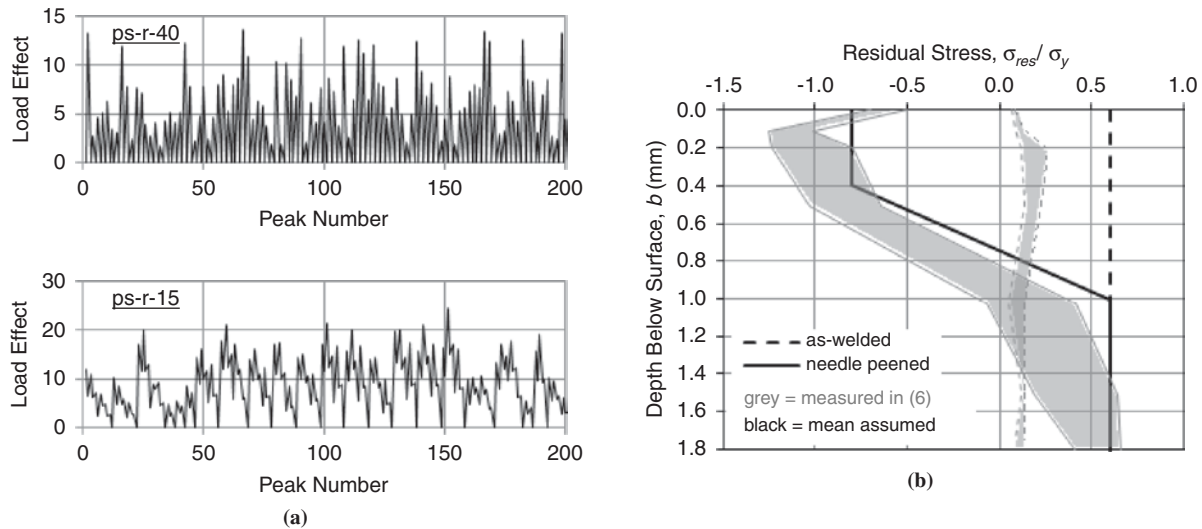


FIGURE 3 Assumed (a) load histories and (b) residual stress distributions.

crack propagation has been studied previously (23, 26, 27). According to Bogdanoff and Kozin, a probability density function of fatigue life derived from testing can be modeled with a high degree of accuracy provided that the transition probabilities and the number of CSs are free to vary (26). In the current study, the number of CSs is fixed and small in number (five CSs are assumed), as would typically be the case in a BMS. The analysis performed for the current study also differs from the previous work in that the possibility is investigated of modifying the transition probability matrix, P , to simulate the effects of postweld treatment by peening after a certain period of time in service.

Calibration of Transition Probabilities

Calibration of the q_i -values for the various CSs was done by first running the probabilistic SBFM model for a given load case and recording at the end of each time increment the probability of the weld's being in each CS. The q_i -values for the Markov chain model were then determined by a least-squares approach (minimizing the errors in the transition probabilities predicted by using the two models). For the current study, this exercise was performed for a number of load cases, for demonstration purposes. Table 4 describes these load cases.

On the basis of earlier work (6), two load histories were examined, which covered a range of loading characteristics likely to be seen in highway bridges (see Figure 3). These histories were generated by

using axle weight and spacing data from a survey in Ontario, Canada (28), along with influence lines for the midspan moment of a 40-m simply supported girder (ps-m-40), and the support reaction for a 15-m simply supported girder (ps-r-15). The resulting loading histories can be characterized as narrow-banded in the ps-m-40 case, with each truck causing a single load cycle, or wide-banded in the ps-r-15 case, with each axle causing a small cycle as it passes onto or off the bridge.

For each history, two stress ranges were investigated: $\Delta S_{eq} = 75$ and 100 MPa. The assumed traffic volumes were 50 or 250 average daily truck traffic (ADTT), corresponding with Class C and D highways in the *Canadian Highway Bridge Design Code* (15). The stress range was taken as the effective stress range, calculated as follows (with $m = 3.0$ assumed):

$$\Delta S_{eq} = \left(\frac{\sum_{i=1}^n N_i \cdot \Delta S_i^m}{N_{total}} \right)^{1/m} \quad (4)$$

where

m = slope of S - N curve,

N_i = number of cycles at stress range i , and

N_{total} = total number of cycles in stress history.

The resulting q_i -values are summarized in Tables 5 and 6 for the ps-m-40 and ps-r-15 loading histories, respectively. The calibration was constrained so that the q_3 - and q_4 -values would not be affected

TABLE 2 Unit Jump Probability Transition Matrix, P

CS at Time t	CS at Time $t + 1$				
	CS1	CS2	CS3	CS4	CS5
CS1	$1 - q_1$	q_1	0	0	0
CS2	0	$1 - q_2$	q_2	0	0
CS3	0	0	$1 - q_3$	q_3	0
CS4	0	0	0	$1 - q_4$	q_4
CS5	0	0	0	0	1

TABLE 3 CS Definitions

Condition State	Critical Crack Depth	
	a_i (mm)	a_c (mm)
CS1	0.10	0.25
CS2	0.25	1.0
CS3	1.0	2.5
CS4	2.5	$T/2$
CS5	$>T/2$	

TABLE 4 Investigated Load Cases

Loading History	Equivalent Stress Range (MPa)	Traffic Volume (ADTT)
ps-m-40	75	50
	75	250
	100	50
ps-r-15	75	50
	75	250
	100	50

by needle peening, on the basis of observations by Ghahremani and Walbridge (6). In general, the q_r -values show similar trends for the two histories. The ps-r-15 history appears to be slightly more severe in most cases for the lower CSs.

In Figure 4, comparisons of the two models are provided for several analysis cases. Specifically, curves of probability versus time are compared for CS1, CS2, and CS5. The selected cases include conditions resulting in both high and low probabilities of being in CS5 at the end of the 100-year analysis period. The agreement between the two models is generally good. There are noticeable differences. However, the simpler Markov chain model captures the overall trends reasonably well.

Modeling of Inspection and Retrofitting

The following expressions are provided by Lassen for the probability of being in a given CS after inspection, given that a repair will definitely occur if a crack exceeding a certain size is detected (23):

$$p_r = \sum_{j=L}^b p_x(j) \cdot p_D(j) \quad (5)$$

$$p'_x(j) = p_x(j) + p_r \cdot p_0(j) \quad \text{for } j = 1, L-1 \quad (6)$$

$$p'_x(j) = p_x(j) \cdot (1 - p_D(j)) + p_r \cdot p_0(j) \quad \text{for } j = L, b \quad (7)$$

where

p_r = probability of repair's occurrence,

$p_0(j)$ = matrix of initial probability of being in each CS,

L = minimum condition state that will trigger repair ($L = 4$ is assumed in this study), and

b = "capturing" or "failure" CS ($b = 5$ in this study).

The following initial probability matrix was established for the current study on the basis of the statistical distribution for the initial crack depth, a_i , assumed in the probabilistic SBFM analysis: $p_0(j) = (0.968, 0.032, 0, 0, 0)$.

Peening after a given period of time in service can be modeled by simply changing the transition probability matrix from the "as-received" to the "peened" matrix in the year that the weld is treated. Implicitly, it is assumed that the peening will not change the current CS. Combinations of inspection, repair, and peening can be considered by simultaneously employing Equations 5 through 7 and changing the transition probability matrix in the year or years that the weld is treated.

ANALYSIS OF FATIGUE MANAGEMENT STRATEGIES

The following fatigue management strategies were analyzed with both models:

- S0. Base case, no inspection (i.e., magnetic particle inspection), repair (i.e., gouging and rewelding), or needle peening;
- S1. Needle peening before the start of the service life;
- S2. Needle peening after 20 years of service loading;
- S3. Inspection and repair (if needed) after 20 years of service loading;
- S4. Inspection, repair (if needed), and needle peening after 20 years of service loading; and
- S5. Inspection, repair, and needle peening as needed after every 20 years of service loading.

A weld repair occurs for Strategies S3–S5 if a crack corresponding with CS4 or CS5 is detected. For Strategy S5, the needle peening would not actually be repeated every 20 years. It would only be carried out after Year 20 immediately following a weld repair if one were to be performed. Figure 5, *a*, *c*, and *e*, presents the analysis results obtained for the ps-m-40 loading history by using the probabilistic SBFM model. On the basis of the results in these plots, the following comments are made:

- After Strategy S1 (needle peening before the start of the service life), Strategy S5 results in the lowest probability of being in CS5, followed by Strategy S4, in all cases.
- In some cases, Strategy S4 is much more effective than Strategy S2, which indicates the importance of inspecting the weld (and repairing it if necessary) before treating it.
- Inspection and repair after 20 years (Strategy S3) results in a reduction in the probability of being in CS5 for a certain period

TABLE 5 Calibrated q_r -Values: Load Case ps-m-40

ΔS_{eq} -ADTT	As-Received Welds			Needle-Peened Welds		
	75–50	75–250	100–50	75–50	75–250	100–50
q_1	0.008696	0.028124	0.021614	0.000000	7.27E-05	0.000178
q_2	0.005826	0.026085	0.014338	2.10E-05	0.000196	0.000440
q_3	0.018445	0.055751	0.032049	0.018445	0.055751	0.032049
q_4	0.020242	0.061971	0.039748	0.020242	0.061971	0.039748

TABLE 6 Calibrated q_i -Values: Load Case ps-r-15

ΔS_{eq} -ADTT	As-Received Welds			Needle-Peened Welds		
	75-50	75-250	100-50	75-50	75-250	100-50
q_1	0.009998	0.040598	0.021092	8.70E-05	0.000690	0.001367
q_2	0.004911	0.024587	0.012071	0.000157	0.002555	0.002710
q_3	0.015718	0.050854	0.029686	0.015718	0.050854	0.029686
q_4	0.016703	0.052903	0.034428	0.016703	0.052903	0.034428

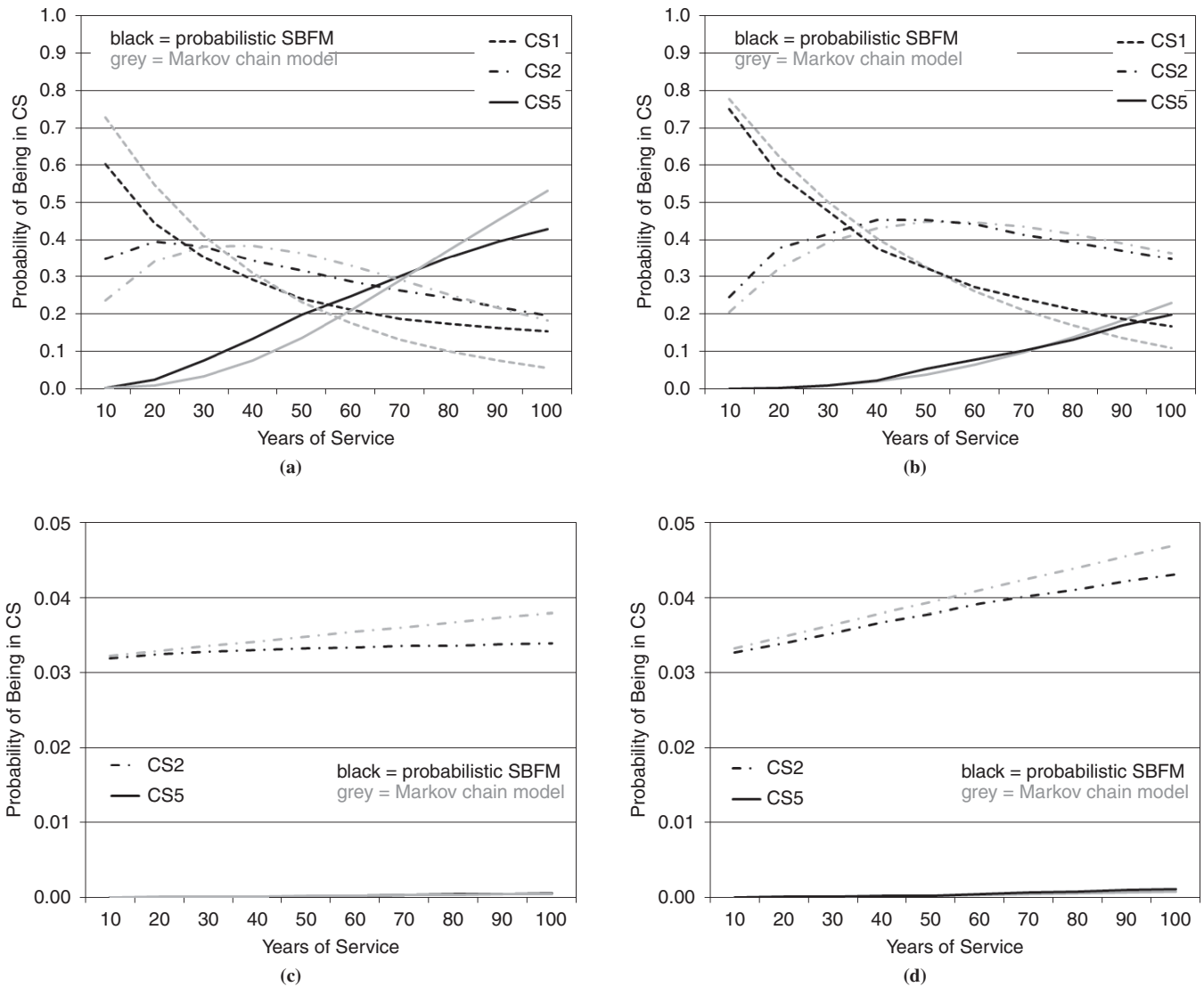
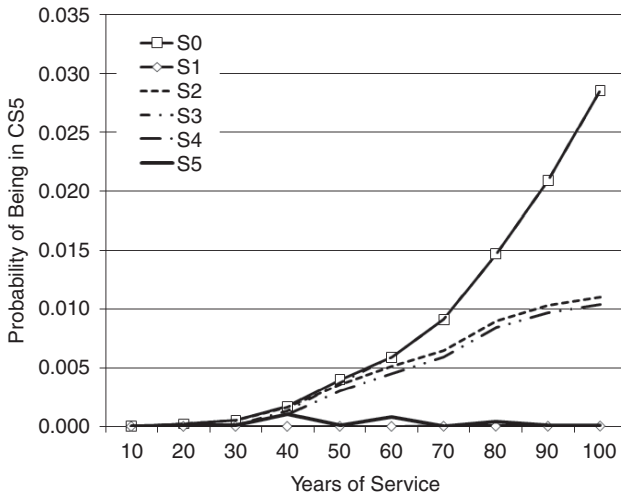
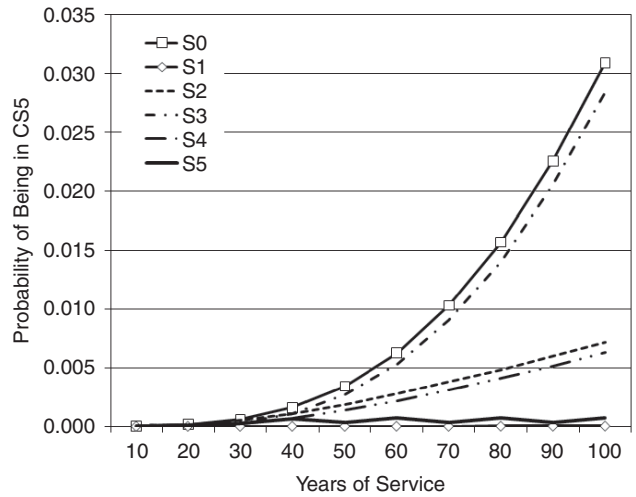


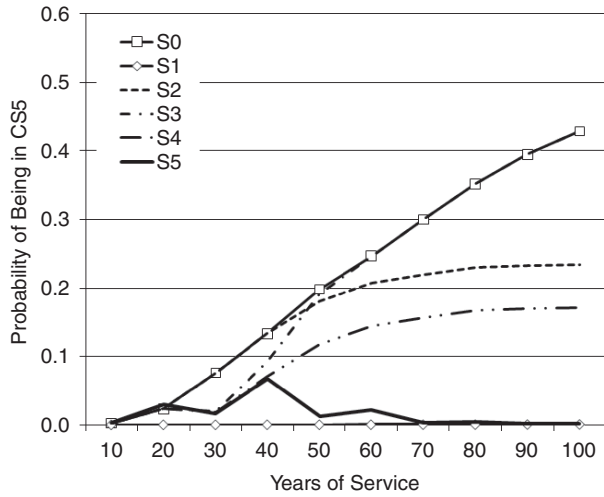
FIGURE 4 Comparison of probabilistic SBFM and Markov chain model predictions: (a) as-received, ps-m-40, $\Delta S_{eq} = 75$ MPa, ADTT = 250; (b) as-received, ps-m-40, $\Delta S_{eq} = 100$ MPa, ADTT = 50; (c) needle peened, ps-m-40, $\Delta S_{eq} = 75$ MPa, ADTT = 250; and (d) needle peened, ps-m-40, $\Delta S_{eq} = 100$ MPa, ADTT = 50.



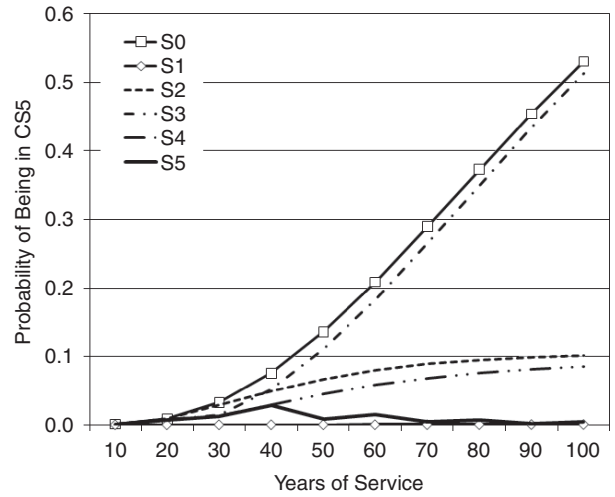
(a)



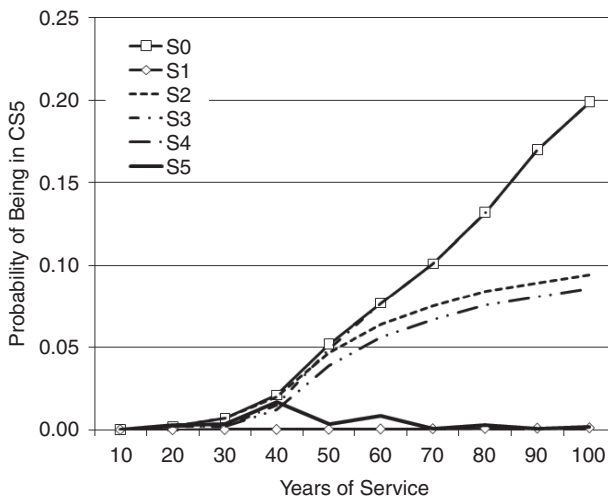
(b)



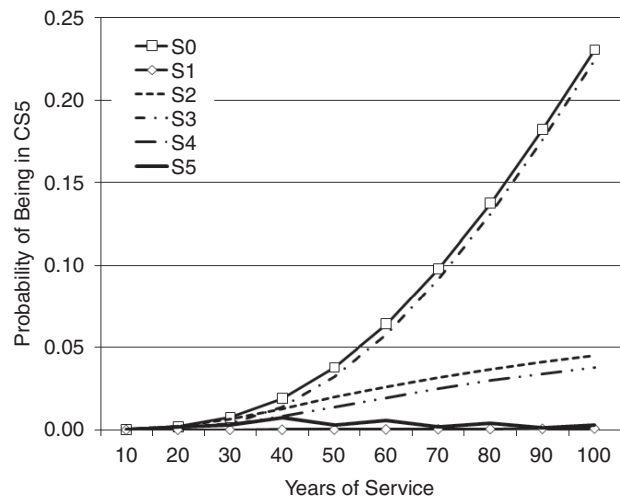
(c)



(d)



(e)



(f)

FIGURE 5 Management strategy comparison: (a) ps-m-40, $\Delta S_{eq} = 75$ MPa, ADTT = 50 (SBFM); (b) ps-m-40, $\Delta S_{eq} = 75$ MPa, ADTT = 50 (Markov); (c) ps-m-40, $\Delta S_{eq} = 75$ MPa, ADTT = 250 (SBFM); (d) ps-m-40, $\Delta S_{eq} = 75$ MPa, ADTT = 250 (Markov); (e) ps-m-40, $\Delta S_{eq} = 100$ MPa, ADTT = 50 (SBFM); and (f) ps-m-40, $\Delta S_{eq} = 100$ MPa, ADTT = 50 (Markov).

of time after Year 20; however, after some time, the curve for this strategy tends to converge on the base case curve (S0).

- With needle peening after 20 years (Strategy S2 or S4), the model predicts a reduction in the probability of being in CS5, which generally does not diminish over time.

COMPARISON OF MODEL PREDICTIONS

In Figure 5, *b*, *d*, and *f*, similar results obtained with the Markov chain fatigue model are presented for comparison purposes. Regarding this comparison, the following comments are made:

- In general, the calibrated Markov chain model captures the general trends well.
- Although there are evidently significant differences in the absolute values in some cases, either model would result in the same ranking of the management strategies.
- Since the Markov chain model in the current study was calibrated to minimize the prediction error for all CSs, there is a larger error in the prediction of being in the failure CS (CS5) than there would be if the calibration procedure had focused on this CS.
- The general trends in Figure 5 were also seen for the ps-r-15 loading history (not shown).

CONCLUSIONS

From the work presented in the previous sections, the following conclusions are drawn:

- Fatigue management strategies in which peening is employed after some period of time in service can result in significant failure probability reductions for bridge welds.
- Peening the weld before loading (Strategy S1) or a maintenance strategy of repeated inspection, repair, and peening during the service life (Strategy S5) results in the lowest probability of being in the failure CS at the end of the analysis period (100 years).
- In general, it is found that peening is more effective if preceded by inspection.
- The Markov chain fatigue model does a reasonable job of predicting the general trends and relative effectiveness of the different investigated management strategies.

Additional work is recommended to further improve the Markov chain fatigue model by investigating other calibration schemes, allowing the number of CSs to vary, and comparing life-cycle cost analysis results wherein the costs associated with all CSs (not just the failure CS) are considered.

REFERENCES

1. *PONTIS Bridge Inspection Manual*. Michigan Department of Transportation, Lansing, 2007.
2. Higashiyama, H., and S. Matsui. Fatigue Durability of Longitudinally Prestressed Concrete Slabs Under Running Wheel (in Japanese). *JSCCE Journal of Structural, Mechanical and Earthquake Engineering*, Vol. 605/I-45, 1998, pp. 79–90.
3. Yokoyama, K., N. Inaba, A. Honma, and N. Ogata. *Development of Bridge Management System for Expressway Bridges in Japan*. PWRI Technical Memorandum No. 4009. Public Works Research Institute, Tsukuba-Shi, Japan, 2006, pp. 99–104.
4. *KUBA-MS-Ticino User's Manual: Release 3.0*. Federal Department of Highways, Bern, Switzerland, 2005.
5. Orcesi, A. D., D. M. Frangopol, and S. Kim. Optimization of Bridge Maintenance Strategies Based on Multiple Limit States and Monitoring. *Engineering Structures*, Vol. 32, 2010, pp. 627–640.
6. Ghahremani, K., and S. Walbridge. Fatigue Testing and Analysis of Peened Highway Bridge Welds Under In-Service Variable Amplitude Loading Conditions. *International Journal of Fatigue*, Vol. 33, 2011, pp. 300–312.
7. Dowling, N. E. *Mechanical Behaviour of Materials*. Pearson Education, Inc., Upper Saddle River, N.J., 2007.
8. Newman, J. C. A Crack Opening Stress Equation for Fatigue Crack Growth. *International Journal of Fracture*, Vol. 24, 1994, pp. R131–R135.
9. Walbridge, S., and A. Nussbaumer. A Probabilistic Assessment of the Effect of Post-Weld Treatment on the Fatigue Performance of Tubular Truss Bridges. *Engineering Structures*, Vol. 30, No. 1, 2008, pp. 247–257.
10. Chen, H., G. Y. Grondin, and R. G. Driver. Characterization of Fatigue Properties of ASTM A709 High Performance Steel. *Journal of Constructional Steel Research*, Vol. 63, No. 6, 2007, pp. 838–848.
11. Chang, S.-T., and F. V. Lawrence. *Improvement of Weld Fatigue Resistance*. Fracture Control Program Report No. 46. University of Illinois, Urbana-Champaign, 1983.
12. Radaj, D., C. M. Sonsino, and D. Flade. Prediction of Service Fatigue Strength of a Welded Tubular Joint on the Basis of the Notch Strain Approach. *International Journal of Fatigue*, Vol. 20, No. 6, 1998, pp. 471–480.
13. Baumel, A., and T. Seeger. *Materials Data for Cyclic Loading—Supplement 1*. Elsevier Science Publishing Company, New York, 1990.
14. Schmidt, B. J., and F. M. Bartlett. Review of Resistance Factor for Steel: Data Collection. *Canadian Journal of Civil Engineering*, Vol. 29, 2002, pp. 98–108.
15. *Canadian Highway Bridge Design Code*. CAN/CSA-S6-06. Canadian Standards Association, Mississauga, Ontario, 2006.
16. *AASHTO LRFD Bridge Design Specifications*. American Association of State Highway and Transportation Officials, Washington, D.C., 2010.
17. *The Manual for Bridge Evaluation: 1st Edition*. American Association of State Highway and Transportation Officials, Washington, D.C., 2008.
18. Monahan, C. C. *Early Fatigue Crack Growth at Welds*. Computational Mechanics Publications, Billerica, Mass., 1995.
19. Fisher, J. W., P. Albrecht, B. T. Yen, D. J. Klingerman, and B. M. McNamee. *NCHRP Report 147: Fatigue Strength of Steel Beams with Welded Stiffeners and Attachments*. TRB, National Research Council, Washington, D.C., 1974.
20. Booth, G. S. Fatigue Life of Ground or Peened Fillet Welded Steel Joints: The Effect of Mean Stress. *Metal Construction*, Vol. 13, 1981, pp. 112–115.
21. Maddox, S. J. Improving the Fatigue Strength of Welded Joints by Peening. *Metal Construction*, Vol. 17, 1985, pp. 220–224.
22. Dürr, A. *Zur Ermüdungsfestigkeit von Schweißkonstruktionen aus höherfesten Baustählen bei Anwendung von UIT-Nachbehandlung*. Doctoral thesis. University of Stuttgart, Stuttgart, Germany, 2006.
23. Lassen, T. Markov Modelling of the Fatigue Damage in Welded Structures Under In-Service Inspection. *International Journal of Fatigue*, Vol. 13, No. 5, 1991, pp. 417–422.
24. Elbehairy, H. *Bridge Management System with Integrated Life Cycle Cost Optimization*. PhD thesis. University of Waterloo, Waterloo, Canada, 2007.
25. Jiang, Y., and K. C. Sinha. Bridge Service Life Prediction Model Using the Markov Chain. In *Transportation Research Record 1223*, TRB, National Research Council, Washington, D.C., 1989, pp. 24–30.
26. Bogdanoff, J. L., and F. Kozin. *Probabilistic Models of Cumulative Damage*. Wiley, New York, 1985.
27. Spencer, B. F., and J. Tang. Markov Process Model for Fatigue Crack Growth. *Journal of Engineering Mechanics*, Vol. 114, No. 12, 1988, pp. 2134–2157.
28. *Commercial Vehicle Survey*. Ministry of Transportation of Ontario, Canada, 1995.